Received: 16 February 2021 | Revised: 3 May 2021 | Accepted: 4 May 2021

DOI: 10.1096/fj.202100286R

RESEARCH ARTICLE

THE FASEB JOURNAL

Endothelial neuropilin-2 influences angiogenesis by regulating actin pattern development and α5-integrin-*p*-FAK complex recruitment to assembling adhesion sites

Christopher J. Benwell[1] | **James A. G. E. Taylor**[1] | **Stephen D. Robinson**[1,2]

[1]Gut Microbes and Health, Quadram Institute Bioscience, Norwich Research Park, Norwich, UK

[2]School of Biological Sciences, University of East Anglia, Norwich Research Park, Norwich, UK

Correspondence
Stephen D. Robinson, Gut Microbes and Health, Quadram Institute Bioscience, Norwich Research Park, Norwich, UK.
Email: Stephen.Robinson@quadram.ac.uk

Funding information
RCUK | Biotechnology and Biological Sciences Research Council (BBSRC), Grant/Award Number: BB/M011216/1; RCUK | Biotechnology and Biological Sciences Research Council (BBSRC), Grant/Award Number: BB/R012490/1; British Heart Foundation (BHF), Grant/Award Number: PG/15/25/31369

Abstract

The ability to form a variety of cell-matrix connections is crucial for angiogenesis to take place. Without stable anchorage to the extracellular matrix (ECM), endothelial cells (ECs) are unable to sense, integrate and disseminate growth factor stimulated responses that drive growth of a vascular bed. Neuropilin-2 (NRP2) is a widely expressed membrane-bound multifunctional non-tyrosine kinase receptor, which has previously been implicated in influencing cell adhesion and migration by interacting with α5-integrin and regulating adhesion turnover. α5-integrin, and its ECM ligand fibronectin (FN) are both known to be upregulated during the formation of neovasculature. Despite being descriptively annotated as a candidate biomarker for aggressive cancer phenotypes, the EC-specific roles for NRP2 during developmental and pathological angiogenesis remain unexplored. The data reported here support a model whereby NRP2 actively promotes EC adhesion and migration by regulating dynamic cytoskeletal remodeling and by stimulating Rab11-dependent recycling of α5-integrin-*p*-FAK complexes to newly assembling adhesion sites. Furthermore, temporal depletion of EC-NRP2 in vivo impairs primary tumor growth by disrupting vessel formation. We also demonstrate that EC-NRP2 is required for normal postnatal retinal vascular development, specifically by regulating cell-matrix adhesion. Upon loss of endothelial NRP2, vascular outgrowth from the optic nerve during superficial plexus formation is disrupted, likely due to reduced FAK phosphorylation within sprouting tip cells.

KEYWORDS
angiogenesis, endothelium, integrins, neuropilin-2, protein trafficking

Abbreviations: CML, chronic myeloid leukemia; DOC, deoxycholate; EC, endothelial cell; ECM, extracellular matrix; EDA-FN, extra domain-A-FN; FA, focal adhesion; FAK, focal adhesion kinase; FN, fibronectin; HUVEC, human umbilical vein endothelial cell; IP, intraperitoneal; MACS, magnetic activated cell sorting; mLMEC, murine lung microvascular endothelial cell; NRP, neuropilin; OHT, tamoxifen; P, postnatal; PIX, β-PAK interacting exchange factor; SC, subcutaneous; VEGF, vascular endothelial growth factor; VEGFR2, VEGF-receptor-2; WT, wild-type.

1 | INTRODUCTION

Angiogenesis, the formation of neo-vasculature from pre-existing blood vessels, is essential to moderate the hypoxic stress that arises in tumor microenvironments.[1] Sustained primary tumor growth therefore relies on the protracted stimulation of neighboring endothelial cells (ECs) to activate appropriate growth factor receptors such as vascular endothelial growth factor (VEGF) receptor-2 (VEGFR2) on their cell surface. The ensuing proliferation and integrin-dependent migration of ECs toward the angiogenic stimulus then results in the formation of a dense network of highly permeable blood vessels to re-perfuse the hypoxic tumor niche.[2]

EC migration relies on the cell's ability to propagate integrin outside-in signaling to the extracellular space.[3-5] Upon ligand binding, integrins mediate the recruitment of core cytosolic scaffolding proteins at the sites of adhesion to the extracellular matrix (ECM) to form focal adhesions (FAs).[6-9] Additional recruitment and clustering of protein kinases such as focal adhesion kinase (FAK) at FAs following integrin-mediated adhesion to the ECM subsequently enables integrin receptors to overcome the limits imposed by the absence of enzymatic or kinase activity in their cytoplasmic tails, allowing for the potentiated activation of numerous signaling cascades.[10] An essential downstream effector for directional cell migration, FAK also indirectly mediates the activation and translocation of Rac1 to FAs, which promotes the nucleation and polymerization of actin stress fibers. This enables for the extension and protrusion of lamellipodia and filopodia at the leading edge to drive cell spreading and migration.[7,11,12] Dynamic remodeling of the actin cytoskeleton is also coupled to the rapid disassembly and re-assembly of nascent FAs, which utilize actin highways to coordinate integrin transport and trafficking.[13-16]

Neuropilin-2 (NRP2) is a single pass transmembrane receptor whose upregulation is consistent with an accelerated cancer progression in a number of cell types (eg, neuroblastomas,[17] non-small-cell lung carcinoma [NSCLC],[18] human prostate carcinoma, melanoma,[19] lung cancer,[20] myeloid leukemia,[21] breast cancer,[22] and pancreatic cancer[23]). As a selective co-receptor for members of the VEGF family of growth factors, the function of NRP2 has also been implicated in influencing EC adhesion, migration and permeability during angiogenesis, under both physiological and pathological conditions.[24-26] NRP2 has since emerged as a promising candidate for targeted therapy against tumorigenesis, however the mechanisms by which it integrates and disseminates ECM and growth factor signals to coordinate EC responses during angiogenesis is as yet unclear.

We have previously shown that endothelial NRP2 drives a VEGF-independent, Rac1-mediated mechanism of cell adhesion and migration over fibronectin (FN) matrices and regulates FA turnover by promoting basal α5-integrin recycling.[24] Here we show that NRP2 regulates VASP-mediated control of actin pattern development to support the protrusion of dynamic lamellipodia at the leading edge of migrating cells. We also elucidate the existence of a NRP2-regulated phospho-FAK (*p*-FAK)-Rab11 trafficking axis, siRNA-mediated depletion of NRP2 in vascular ECs dampening the activation and recruitment of *p*-FAK to α5-integrin containing adhesions. We build on our previous work by demonstrating that the reduction in FA turnover rate elicited by NRP2 silencing leads to an accelerated growth of tensin-1 positive fibrillar adhesions, which in turn promotes FN fibrillogenesis. Finally, by utilizing a mouse model that expresses a tamoxifen-inducible Cre-recombinase under the control of a PDGFb promoter, we examine the effects of specifically and temporally depleting endothelial NRP2 in vivo. To this end we demonstrate that loss of endothelial NRP2 inhibits tumorigenesis, and transiently impairs physiological vascularization of developing postnatal retinae. This work highlights the advantages of employing endothelial-specific targeting therapies against pathological angiogenesis, in addition to providing further evidence that NRP2 is a promising anti-angiogenic target to impair primary tumor growth.

2 | MATERIALS AND METHODS

2.1 | Animal generation

NRP2 floxed ($NRP2^{flfl}$) mice were purchased from Jackson Laboratories (Bar Harbour, Maine, USA), and were generated by gene target insertion of embryonic stem cells, resulting in the insertion of loxP sites flanking exon 1 of the NRP2 gene. A loxP-tauGFP FRT-flanked neo cassette was inserted 1 kb into intron 1 *via* homologous recombination. Heterozygous animals were crossed to an flp recombinase transgenic line for removal of the neo cassette. The PCR analysis to confirm floxing was carried out using the following oligonucleotide primers:

Forward (WT) primer (Reaction A): 5′-CAGG TGACTGGGGATAGGGTA-3′

Common primer (Reaction A + B): 5′-AGCTT TTGCCTCAGGACCCA-3′

Forward primer (^{flfl}) (Reaction B): 5′-CCTGA CTACTCCCAGTCATAG-3′

Transgenic mice expressing a tamoxifen-inducible PDGFb-$iCreER^{T2}$ allele in vascular ECs were provided by Marcus Fruttiger (UCL, London, UK), and were generated by substituting the exon 1 of the PDGFb gene by the $iCreER^{T2}$-IRES-EGFP-pA sequence.

Forward primer: 5′-GCCGCCGGGATCACTC TC-3′

Reverse primer: 5′-CCAGCCGCCGTCGCAA CT-3′

NRP2^{flfl} mice were bred with PDGFb.iCreER^{T2} mice to generate NRP2^{flfl}; PDGFb.iCreER animals. PDGFβ-iCreERT2 expression was maintained exclusively on breeding males, thereby ensuring the generation of both Cre-negative and positive offspring and enabling the use of littermate controls. All animals were bred on a pure C57/BL6 background.

2.2 | Cell isolation, immortalization, and cell culture

Primary mouse lung microvascular endothelial cells (mLMECs) were isolated from adult mice bred on a pure C57/BL6 background. Primary ECs were twice positively selected for through their expression of endomucin by magnetic activated cell sorting (MACS) as previously described by Reynolds and Hodivala-Dilke.[27] ECs were immortalized using polyoma-middle-T-antigen (PyMT) retroviral transfection as previously described by Robinson et al[28] Immortalized mLMECs were cultured in IMMLEC media, a 1:1 mix of Ham's F-12:DMEM medium (low glucose) supplemented with 10% FBS, 100 units/mL penicillin/streptomycin (P/S), 2 mM glutamax, 50 μg/mL heparin (Sigma).

Immortalized mLMECs were cultured on 0.1% gelatin coated flasks at 37°C in a humidified incubator with 5% CO_2. For experimental analyses, plates, dishes and flasks were coated in 10 μg/mL human plasma fibronectin (FN) (Millipore) overnight at 4°C. Vascular endothelial growth factor-A (VEGF-A_{164}: mouse equivalent of VEGF-A_{165}) was made in-house as previously described by Krilleke et al.[29]

2.3 | siRNA transfection

ECs were transfected with non-targeting control siRNA or a mouse-specific NRP2 siRNA construct (Dharmacon), suspended in nucleofection buffer (200 mM Hepes, 137 mM NaCl, 5 mM KCl, 6 mM D-glucose, and 7 mM Na_2HPO_4 in nuclease-free water; filter sterilized) using the Amaxa 4D-nucleofector system (Lonza) under nucleofection program EO-100, according to manufacturer's instructions.

2.4 | Immunocytochemistry

siRNA-transfected ECs were seeded onto FN-coated acid-washed, oven sterilized glass coverslips in 24-well plates at a seeding density of 2.5×10^4 cells/well. ECs were fixed at indicated timepoints in 4% paraformaldehyde (4% PFA) for 10 minutes, washed in PBS, blocked and permeabilized with 10% goat serum, PBS 0.3% triton X-100 for one hour at room temperature. Cells were incubated in primary antibody in PBS overnight at 4°C. Primary antibodies were: anti-α5-integrin (clone ab150361; Abcam), anti-p- FAK^{Tyr407} (clone 44-650G Invitrogen), anti-Rab11 (clone 3612; Abcam), anti-tensin-1 (clone NBP1-84129; Novus Biologicals), EDA-FN (F6140; Sigma). Coverslips were PBS washed, and incubated with an appropriate Alexa fluor secondary antibody diluted 1:200 in PBS for two hours at room temperature. F-actin staining was performed by incubating cells in phalloidin-364 diluted 1:40 in PBS for 2 hours at room temperature during secondary antibody incubation. Coverslips were PBS washed again, before being mounted onto slides with Prolong Gold containing DAPI (Invitrogen). Images were captured either using a Zeiss AxioImager M2 microscope (AxioCam MRm camera) at 63x magnification or using a Zeiss LSM880 Airyscan Confocal microscope at 63X magnification. FA number and size, and EDA-FN fibers/cell were quantified using ImageJ software as previously described by Lambert et al[30] XZ confocal sections taken across the z-plane were processed to form a 2D projection representing the full depth of the cell culture.

2.5 | Western blot analysis

siRNA transfected ECs were seeded into FN-coated six-well plates at a seeding density of 5×10^5 cells/well and incubated for 48 hours at 37°C in a 5% CO_2 incubator. ECs were lysed in electrophoresis sample buffer (ESB) (Tris-HCL: 65 mM pH 7.4, sucrose: 60 mM, 3% SDS), and homogenized using a Tissue Lyser (Qiagen) with acid-washed glass beads (Sigma). Following protein quantification using the DC BioRad assay, 30 μg of protein from each sample was loaded onto 8% polyacrylamide gels and subjected to SDS-PAGE. Proteins were transferred to a nitrocellulose membrane (Sigma) and incubated in 5% milk powder in PBS 0.1% Tween-20 (0.1% PBST) for 1 hour at room temperature followed by an overnight incubation in primary antibody diluted 1:1000 in 5% bovine serum albumin (BSA) in 0.1% PBST at 4°C. Membranes were washed 3x with 0.1% PBST and incubated in an appropriate horseradish peroxidase (HRP)-conjugated secondary antibody (Dako) diluted 1:2000 in 5% milk powder in 0.1% PBST for two hours at room temperature. Membranes were washed again 3x with 0.1% PBST before being incubated with a 1:1 solution of Pierce ECL Western Blotting Substrate (Thermo Scientific). Chemiluminescence was detected on a ChemiDoc MP Imaging System darkroom (BioRad). Densitometric readings of band intensities for blots were obtained using ImageJ. Primary antibodies (all used at 1:1000

dilution and purchased from Cell Signalling Technology, unless noted otherwise) were: anti-NRP2 (clone D39A5), anti-HSC70 (clone B-6; Santa Cruz Biotechnology), anti-p-VASP^{Ser157} (clone 3111), anti-VASP (clone 3132), anti-p-FAK^{Tyr407} (clone 44-650G; Invitrogen), anti-tensin-1 (clone NBP1-84129; Novus Biologicals), anti-GAPDH (60004-1-1g; Proteintech), EDA-FN (F6140; Sigma).

2.6 | Signaling assays

siRNA-transfected ECs were seeded into FN-coated 6 cm cultures dishes at a density of 5×10^5 cells/well and incubated for 48 hours. ECs were then PBS washed and starved for 3 hours in serum free medium (OptiMEM; Invitrogen). VEGF was then added at a final concentration of 30 ng/mL at indicated timepoints. ECs were then subjected to lysing, protein quantification and protein expression analysis by Western blot.

2.7 | Co-immunoprecipitation assays

siRNA-transfected ECs were seeded into FN-coated 10 cm dishes at a density of 2×10^6 cells/dish, and incubated for 48 hours. ECs were then lysed on ice in lysis buffer as previously described by Valdembri et al[16] in the presence of 100X Halt protease inhibitor cocktail (Thermo Scientific) and protein quantified using the DC BioRad assay. 200 μg protein from each sample was immunoprecipitated by incubation with protein-G Dynabeads (Invitrogen) coupled to a rabbit anti-α5-integrin antibody (clone 4705S, Cell Signalling Technology) on a rotator overnight at 4°C. Immunoprecipitated complexes were then washed 3x with lysis buffer + 100X Halt protease inhibitor, and once in PBS, before being added to and boiled in NuPAGE sample reducing agent and sample buffer (Life Technologies) for Western blot analysis.

2.8 | Deoxycholate (DOC) buffer-extraction

siRNA-treated ECs were allowed to adhere for 16 hours at 37°C and 5% CO_2. ECs were then lysed in DOC lysis buffer (20mM Tris, pH 8.5, 1% sodium deoxycholate, 2mM iodoacetamide, 2mM EDTA) in the presence of 100X Halt protease inhibitor cocktail, cleared by centrifugation, and the insoluble fraction isolated. Insoluble fractions were separated by SDS-PAGE and subjected to western blot analysis.

2.9 | In vivo CMT19T tumor growth assays

Inducible, endothelial specific deletion of NRP2 was achieved by crossing mice expressing the PDGFb.iCreER promoter of Cre-recombinase to those floxed for NRP2. NRP2^{flfl}; PDGFb.iCreER and NRP2^{flfl} littermate control mice received intraperitoneal (IP) injections of tamoxifen (75 mg/kg bodyweight, 2 mg/mL stock) thrice weekly (Monday, Wednesday, and Friday) for the duration of the experiment from D4 to D17 to induce Cre-recombinase activity. CMT19T lung carcinoma cells (CR-UK Cell Production) (1×10^6) were implanted subcutaneously (SC) into the flank of mice at D0 and allowed to grow until D18. On D18, mice were killed, tumor sizes measured, and tumor samples fixed in 4% PFA for blood vessel density analysis. Tumor volumes were calculated according to the formula: length x width^2 x 0.52.

2.10 | Immunofluorescence analysis of tumor sections

Tumor sections were fixed in 4% PFA for 10 minutes at RT before being washed twice in PBS 0.3% triton-X100, twice in PBLEC (1x PBS, 1% Tween 20, 0.1 mM $CaCl_2$, 0.1 mM $MgCl_2$, 0.1 mM $MnCl_2$) and incubated in Dako protein block serum free (Agilent). Sections were then incubated overnight at 4°C in primary antibodies against NRP2 (clone Sc-13117; Santa-Cruz Biotechnology) and endomucin (clone Sc-65495; Santa-Cruz Biotechnology). Following primary antibody incubation, sections were washed again twice in PBS 0.3% triton-X100 and PBLEC before being incubated in the appropriate Alexa fluor secondary antibody for two hours at RT. Sections were then blocked in Sudan black for 5 minutes before being mounted with flouromount + DAPI and imaged at 10X magnification using a Zeiss AxioImager M2 microscope (AxioCam MRm camera). Blood vessel density was assessed by counting the number of endomucin-positive vessels per mm^2 from three representative ROIs/ section, averaged over three sections/tumor.

2.11 | In vivo retina assays

Inducible, endothelial specific deletion of NRP2 was achieved by crossing mice expressing the PDGFb.iCreER promoter of Cre-recombinase to those floxed for NRP2. Tamoxifen-induced activation of Cre-recombinase and thus deletion of NRP2 was employed via 2 regimes: NRP2^{flfl}; PDGFb.iCreER and NRP2^{flfl} littermate control mice either received subcutaneous (SC) injections of tamoxifen (50 μL, 2 mg/mL stock) on postnatal (P) days 2 and 3, followed by intraperitoneal (IP) injections of the same dose on P4 and 5 before retinas being harvested at P6, or mice received IP injections of tamoxifen (50 μL, 2 mg/mL stock) on postnatal (P) days 7 to 10 before retinas being harvested at P12. After dissection, retinas were fixed in ice-cold methanol for 30 minutes before being prepared

for blocking and immunostaining. First, retinas were permeabilized in PBS 0.25% triton-X100 for 30 minutes at RT, before being washed twice in PBLEC and then blocked in Dako protein block serum free for one hour. Retinas were then incubated in primary antibodies against: FITC-BS-1 lectin (clone L2895; Sigma), NRP2 (clone Sc-13117; Santa-Cruz Biotechnology), αSMA (clone Ab21027; Abcam), ERG 1 / 2 (clone Ab92513; Abcam), p-FAK^{Tyr407} (clone 44-650G Invitrogen), Collagen IV (clone Ab19808; Abcam). Following primary antibody incubation, retinas were incubated in the appropriate Alexa fluor secondary antibody for 1 hour at RT, before being washed twice in PBS 0.1% triton-X100 and mounted. Images were captured using a Zeiss LSM880 Airyscan Confocal microscope. Vascular extension analysis was performed using ImageJ, vessel density analysis was performed using AngioTool.

2.12 | Statistical analysis

The graphic illustrations and analyses to determine statistical significance were generated using GraphPad Prism 6 software and Student's *t* tests, respectively. Bar charts show mean values and the standard error of the mean (+SEM). Asterisks indicate the statistical significance of *P* values: $P > .05$ = NS (not significant), * $P < .05$, ** $P < .01$, *** $P < .001$ and **** $P < .0001$.

3 | RESULTS

3.1 | VASP-mediated actin pattern development is sensitive to the loss of NRP2

Angiogenesis relies on the ability of ECs to sense, integrate and disseminate signals they receive from the ECM and from secreted growth factors in order to adhere and migrate toward the angiogenic stimulus.[31,32] We have previously used multiple specific NRP2 siRNAs in both immortalized and primary mouse-lung microvascular ECs (mLMECs) to identify endothelial NRP2 as a key regulator of EC adhesion and migration by promoting FA turnover and Rac1 activation, independent of VEGF-stimulation. Label-free quantitative mass spectrometry was additionally utilized to elucidate candidate NRP2 interactions with several endocytic and recycling-associated trafficking proteins.[24]

Migrating cells rely on the stimulation of numerous canonical signaling networks that converge on the organized remodeling of the cytoskeleton.[33] Actin is the major cytoskeletal element in ECs, and continuously undergoes stress fiber remodeling into [protrusions to maintain the cell in a motile state.[7,12,34] Given NRP2's regulation of Rac1 activity, we decided to consider its involvement during actin cytoskeletal remodeling in mLMECs. Luo et al, recently reported that pancreatic neuroendocrine tumor (PNET)-associated human umbilical vein ECs (HUVECs) ectopically overexpressing NRP2 formed larger actin-rich lamellipodial protrusions at the cell periphery compared to control ECs. This was subsequently shown to result from an upregulation of cofilin activity, propagating increased rates of actin polymerization at the leading edges of the cell.[35] To investigate whether NRP2 is dispensable for actin cytoskeletal remodeling during initial adhesion to the ECM, we allowed control (*si*Ctrl) and NRP2-siRNA (*si*NRP2)-treated ECs to adhere to FN for 90 minutes before fixation and stained for filamentous actin (Figure 1A). While Ctrl ECs formed long linear stress fibers ending in actin-rich lamellipodial protrusions, NRP2 siRNA-treated ECs appeared more circular, with visibly fewer linear stress fibers, protrusions and actin microspikes (Figure 1B). A similar observation was reported by Fantin et al, following NRP1 knockdown in hMVECs, delineating a role for NRP1 in the regulation of Rac1-mediated actin pattern development.[36,37]

To further elucidate the mechanisms by which NRP2 controls the remodeling of the actin cytoskeleton, we re-examined our label-free mass spectrometry data, originally performed to take an unbiased approach to identifying candidate proteins associating with NRP2 in mLMECs.[24] This re-analysis revealed a large number of proteins known to be involved in regulating the actin cytoskeleton. Of note, this included those known to stabilize the spectrin actin network such as tropomyosin-1, members of the Arp2/3 complex, including cortactin, which regulates branch nucleation and polymerization, and proteins involved in coordinating stress fiber development, such as VASP, cofilin-1, fascin, and TRIO-binding protein.[35,38-40] Unlike cofilin proteins, VASP functions as a potent regulator of both radial fiber formation and chiral actin pattern development, its depletion in fibroblasts preventing the transition from initial actin-rich peripheral rings to long linear stress fibers that support growth of dynamic protrusions.[41,42] As NRP2 depletion appeared to impair the formation of linear stress fibers, we next investigated whether NRP2 regulates VASP activity by monitoring total and phosphorylated VASP expression in the presence or absence of VEGF stimulation. While total VASP expression was unaltered following NRP2 siRNA treatment, NRP2 depletion elicited a reduction in VASP phosphorylation at residue Ser157 at both 5 and 15 minutes post VEGF stimulation (Figure 1C,D). Phosphorylation at Ser157 provides a signal for membrane or leading-edge localization of VASP,[41,43] enabling its interaction with FA-associated proteins such as FAK, which have important roles in potentiating Rac1 activation and translocation to newly forming focal adhesions at the leading edges of cells.[11,44] Taken together, these results suggest that NRP2's modulatory role over Rac1 during focal adhesion assembly is dependent upon its ability to promote VASP-mediated actin remodeling.

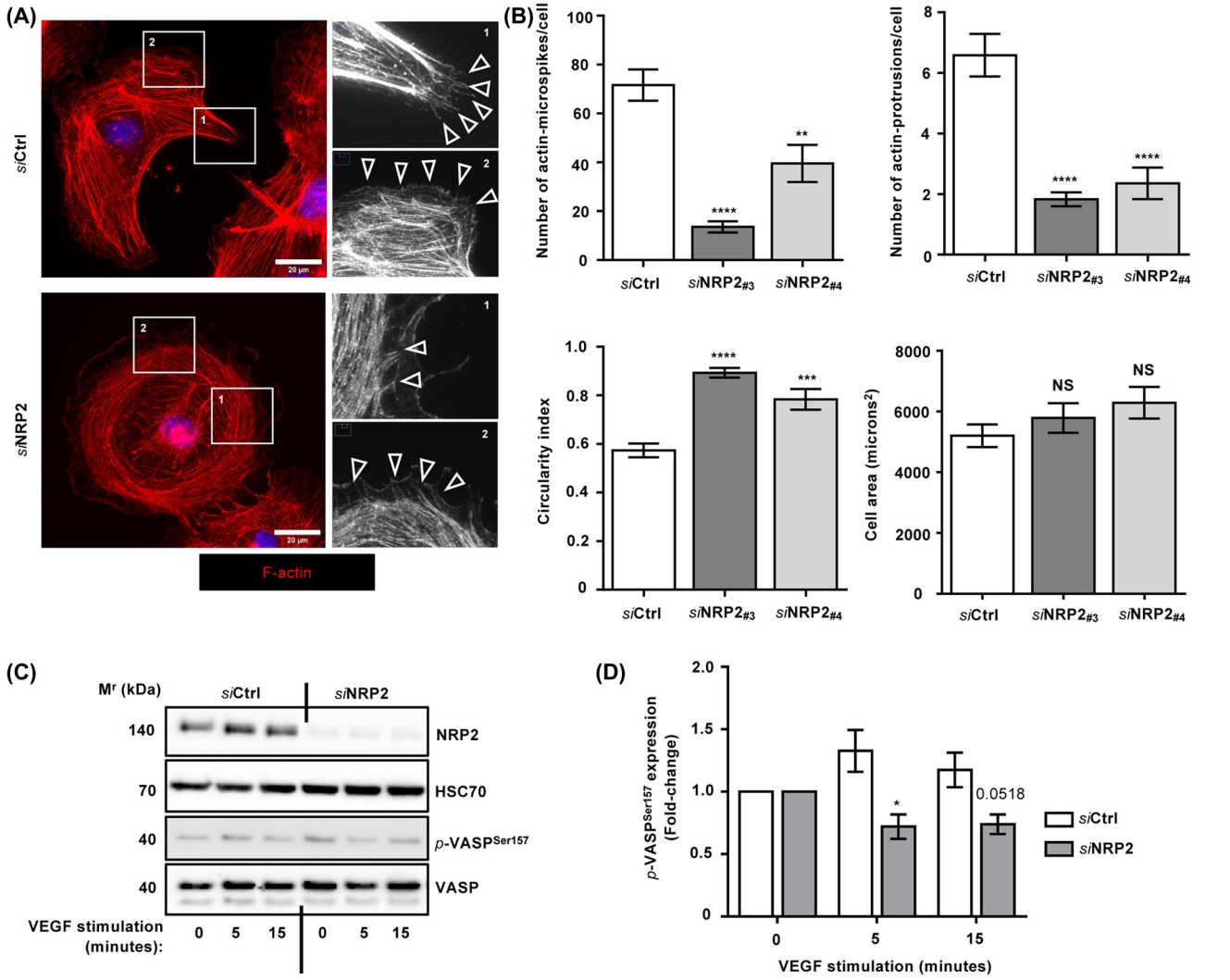

FIGURE 1 VASP-mediated actin pattern development and FAK phosphorylation are sensitive to the loss of NRP2. A, siRNA-transfected ECs were seeded onto FN coated coverslips and allowed to adhere for 90 min at 37°C and 5% CO_2 before being fixed. ECs were then stained for filamentous actin using phalloidin Alexa Fluor 568. Images were taken using a Zeiss AxioImager M2 microscope at 63X magnification. Arrowheads point to actin microspikes at cell periphery. B, Quantification of number of actin microspikes and actin protrusions/cell, cell circularity calculated as 4PiArea/Perimeter^2, and cell area (microns^2) in Ctrl siRNA and NRP2 siRNA-treated ECs. Two separate NRP2-targeting siRNAs (#3 and #4) were tested to confirm results. Error bars show ±SEM; n ≥ 15 cells/siRNA-treated group. Asterisks indicate statistical significance from an unpaired two-tailed *t* test. C, siRNA-transfected ECs were seeded onto FN and allowed to adhere for 48 h at 37°C and 5% CO_2. ECs were subsequently starved in serum-free medium and stimulated with VEGF (30 ng/mL) for the indicated time. EC extracts were immunoblotted using antibodies against NRP2, HSC70, phospho-VASP (*p*-VASP) (Ser157) and VASP. Panel shows representative western blot image. D, Densitometric quantification of mean *p*-VASP (Ser157) band intensities normalized against total VASP expression and obtained using ImageJ. Error bars show ±SEM; N = 3 independent experiments. Asterisks indicate statistical significance from an unpaired two-tailed *t* test (compared to *si*Ctrl)

3.2 | NRP2 promotes FAK phosphorylation and recruitment to assembling focal adhesion sites in ECs

We next considered whether NRP2 depletion would impair FAK phosphorylation. NRP2 has been demonstrated to localize to *p*-FAK-positive adhesions in breast-tumor epithelial cells allowed to adhere on laminin matrices,[45] and to regulate FAK signaling during branching morphogenesis in the developing mammary gland.[46] It is however unclear whether NRP2 influences FAK-mediated responses in microvascular ECs during angiogenesis. Following VEGF stimulation, FAK undergoes autophosphorylation at its Tyr^{397} residue, exposing binding sites for Src family kinases, which are involved in phosphorylating additional sites on FAK such as Tyr^{407}.[47,48] Both residues have been implicated in promoting EC migration and adhesion by potentiating the activation of downstream signaling cascades, such as the β-PAK

interacting exchange factor (PIX)-dependent activation of Rac1.[11] To assess whether NRP2 regulates FAK phosphorylation at either Tyr^{397} or Tyr^{407} in mLMECs adhered to FN, we assessed the expression of total and *p*-FAK in a similar manner as described above for VASP. At 5 minutes VEGF stimulation, NRP2 depleted ECs exhibited a less robust pattern of FAK phosphorylation at both Tyr^{397} and Tyr^{407} compared to Ctrl ECs (Figures S1A,B and S2A,B).

Tethering of α5-integrin to FN at assembling adhesion sites is required for initial FAK recruitment, aggregation and phosphorylation during nascent FA formation.[48,49] We have previously shown that NRP2 interacts with and regulates the recycling of α5-integrin in ECs to promote the assembly of FAs at the leading edge.[24] As NRP2 depletion impaired FAK phosphorylation, we sought to determine whether NRP2 also regulates the recruitment of FAK to assembling α5-integrin adhesions. As NRP1 disseminates VEGF-mediated signaling via the phosphorylation of FAK at Tyr^{407},[47] we focused on how NRP2 regulates the interactions between α5-integrin and this residue specifically by immunofluorescence confocal microscopy. To this end, we examined the colocalization between *p*-FAK^{Tyr407} and α5-integrin in Ctrl or NRP2-siRNA treated ECs allowed to adhere to FN for 90 minutes. While Ctrl ECs exhibited a strong colocalizationz between α5-integrin and *p*-FAK^{Tyr407} around the cell periphery within large characteristic adhesion structures, NRP2 depleted ECs displayed smaller α5-integrin adhesions, and those present were less enriched in *p*-FAK^{Tyr407}. In addition, in NRP2 depleted cells we observed an increased accumulation of *p*-FAK^{Tyr407} around the perinuclear region (Figure 2C-E). To confirm that these differences did not arise as an artifact of cell immortalization, we quantified the mean adhesion size in wild-type (WT)-derived primary and immortalized ECs adhered to FN for 90 minutes; we observed no significant alterations (Figure 2F). To corroborate these findings, we biochemically assessed the physical interaction between α5-integrin and *p*-FAK^{Tyr407} in Ctrl and NRP2 siRNA-treated ECs by co-immunoprecipitation. Lysate collected from Ctrl ECs displayed a more robust interaction between α5-integrin and *p*-FAK^{Tyr407} compared to lysate collected from NRP2 depleted ECs (Figure 2G), confirming that NRP2 is required for the proper recruitment and phosphorylation of FAK during FA assembly.

3.3 | NRP2 regulates an α5-integrin-*p*-FAK^{Tyr407}-Rab11 trafficking axis

Studies have revealed that the retention of *p*-FAK within endocytosing integrin complexes, including subsequent Rab11-associated recycling, sustains the active integrin conformation, enabling enhanced polarized reassembly of nascent FAs at the leading edge of the cell.[34] We have previously provided evidence that NRP2 forms associations with Rab11 to facilitate α5-integrin recycling.[24] As NRP2 depletion impaired the recruitment and phosphorylation of FAK to α5-integrin adhesion sites, we sought to determine whether NRP2 regulates an α5-integrin-*p*-FAK-Rab11 recycling axis to promote FA assembly and development. To examine this, we first stained for both Rab11 and NRP2 to ascertain their colocalization in mLMECs. NRP2 colocalized with Rab11 at both the perinuclear region of the cell, and within trafficking vesicles (Figure S2A), confirming our previous co-immunoprecipitation studies and suggesting a physical interaction.

To visualize the functional consequences of NRP2 silencing on Rab11-associated trafficking, we co-immunolabeled Rab11 with endogenous *p*-FAK^{Tyr407} or α5-integrin in Ctrl or NRP2 siRNA-treated ECs allowed to adhere on FN for 90 minutes. As before, with NRP2 knockdown we observed a significant accumulation of *p*-FAK^{Tyr407} arresting within the perinuclear region of the cell, and a weaker colocalization with fewer $Rab11^+$ vesicles undergoing recycling back to assembling adhesion sites at the periphery of the cell (Figure 3A,C-E). Furthermore, NRP2 depleted ECs exhibited a dramatic un-coupling of α5-integrin with $Rab11^+$ vesicles at both the perinuclear region and at the cell periphery (Figure 3B,C,F). These data suggest that NRP2 regulates Rab11-facilitated transport of both α5-integrin and *p*-FAK in ECs. Upon NRP2 silencing, assembling nascent adhesions are smaller, resulting from a reduced rate of α5-integrin recycling and *p*-FAK^{Tyr407} recruitment, concomitant with the accumulation of both α5-integrin and *p*-FAK^{Tyr407} at the perinuclear region.

3.4 | Long term depletion of NRP2 accelerates FA maturation and fibrillogenesis

As FAs mature and become influenced by actomyosin-driven forces, their composition transitions from small highly tyrosine phosphorylated focal contacts, to large macromolecular assemblies.[50,51] While focal contacts often translocate by extending centripetally and contracting peripherally, and are rapidly turned over to promote migration, mature FA complexes anchor to the actin cytoskeleton to mediate more stable mechanical changes within the cell. Stress-fiber-associated FAs can further mature into fibrillar adhesions after approximately 24 hours, whereby engaged α5β1-integrin is translocated along actin cables centripetally toward the cell body. These elongated beaded structures become increasingly enriched with the actin-binding protein tensin-1 as they extend from the medial ends of the stationary FA, and act to funnel the necessary actomyosin tension required to unfold and integrate secreted FN dimers into an extracellular fibrillar network.[52,53] Fibrillar adhesion formation is

therefore characteristic of a reduced motility and increased cell stability.

Since NRP2 promotes initial FA organization and development by regulating Rab11-mediated trafficking of α5-integrin and FAK, we considered whether its protracted depletion would continue to impair FA maturation. Surprisingly, NRP2 siRNA-treated ECs adhered to FN for 180 minutes and 16 hours exhibited significantly larger α5-integrin positive adhesions than their Ctrl siRNA-treated counterparts (Figure 4A). While Ctrl siRNA-treated ECs fixed at 16 hours exhibited mature, α5-integrin adhesions at the cell periphery, NRP2 depleted ECs displayed a high density of characteristic, tensin-1 positive

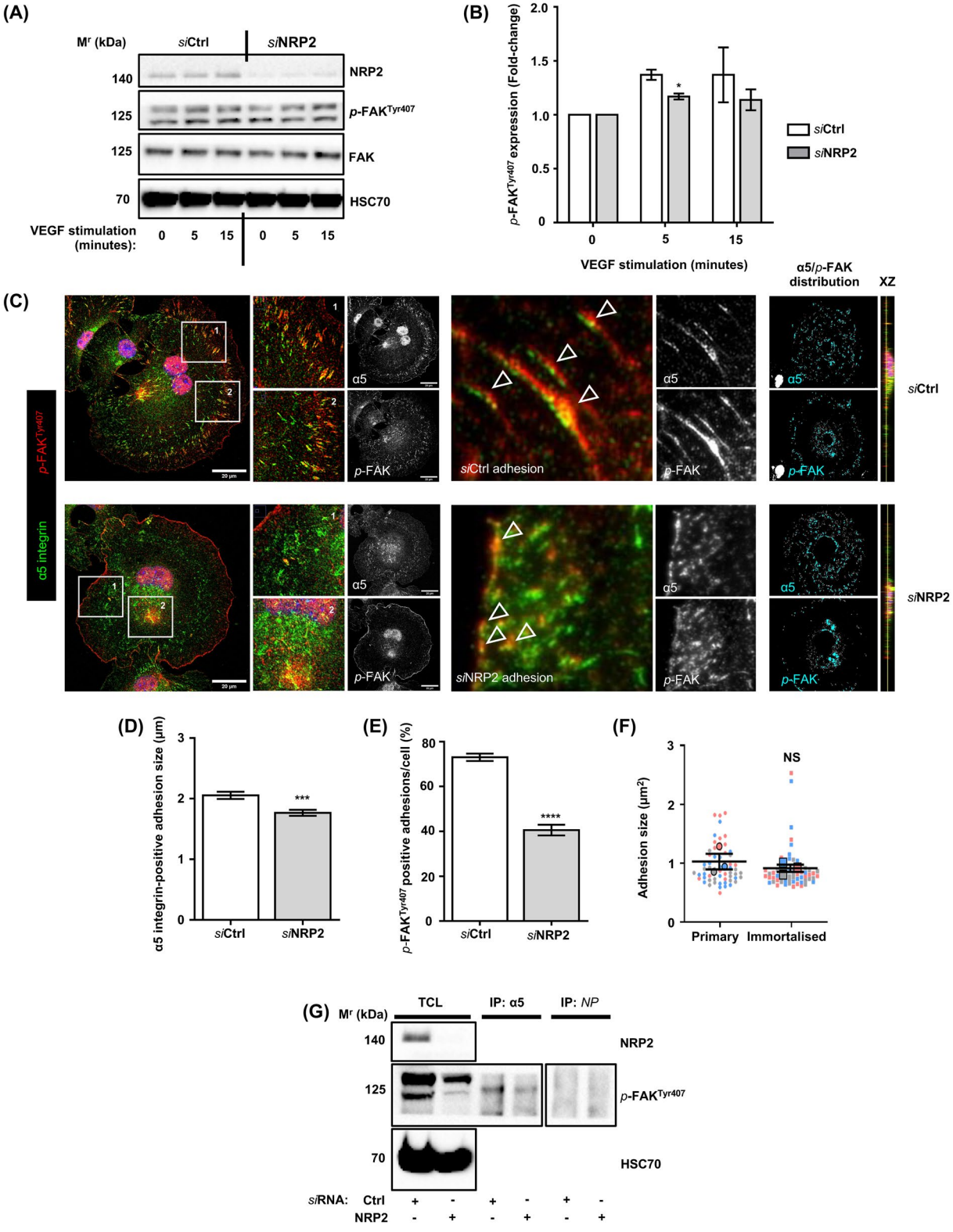

FIGURE 2 NRP2 promotes FAK phosphorylation and recruitment to assembling focal adhesion sites in ECs. A, siRNA-transfected ECs were seeded onto FN and prepared as described in Figure 1D. EC extracts were immunoblotted using antibodies against NRP2, *p*-FAK (Tyr407), FAK and HSC70. Panel shows representative western blot image. B, Densitometric quantification of mean *p*-FAK band intensities normalized against total FAK expression and obtained using ImageJ. Error bars show ±SEM; N = 3 independent experiments. Asterisks indicate statistical significance from an unpaired two-tailed *t* test. C, siRNA-transfected ECs were seeded onto FN coated coverslips and allowed to adhere for 90 min at 37°C and 5% CO_2 before being fixed. ECs were then co-immunostained for α5-integrin and *p*-FAK (Tyr407). Images were taken using a Zeiss LSM880 Airyscan Confocal microscope at 63X magnification. Arrowheads show colocalization at peripheral adhesions. XZ plane images for each panel are also shown to display subcellular colocalization. D, Quantification of mean α5-integrin positive adhesion size (microns) between Ctrl siRNA and NRP2 siRNA-treated ECs. Error bars show ±SEM; N = 3 independent experiments; n ≥ 180 adhesions/siRNA-treated group. Asterisks indicate statistical significance from an unpaired two-tailed *t* test. E, Quantification of % of *p*-FAK (Tyr407)-positive α5-integrin adhesions per cell between Ctrl siRNA and NRP2 siRNA-treated ECs. Error bars show ±SEM; N = 3 independent experiments; n ≥ 30 cells/siRNA-treated group. Asterisks indicate statistical significance from an unpaired two-tailed *t* test. F) Superplot showing quantification of mean adhesion area (microns^2) per cell between primary and immortalized mLMECs. Error bars show ±SEM; N = 3 independently derived EC clones (points from each biological replicate are shown as a different color where the mean value for each replicate is shown as a larger circle of the same color); n ≥ 60 cells/ group. NS=not significant from an unpaired two-tailed *t* test. G, siRNA-transfected ECs were seeded onto FN and allowed to adhere for 48 h at 37°C and 5% CO_2. EC extracts were immunoprecipitated by incubation with protein-G Dynabeads coupled to a α5-integrin antibody. Immunoprecipitated complexes were subjected to western blot analysis using antibodies against *p*-FAK (Tyr407). NRP2 silencing was confirmed by subjecting the total cell lysate to western blot analysis and incubating blots in antibodies against NRP2 and HSC70

fibrillar adhesions. Confocal XZ sectioning subsequently confirmed the colocalization between endogenous α5-integrin and tensin-1 at the cell body in ECs depleted of NRP2, while in our Ctrl ECs tensin-1 exclusively co-localized with α5-integrin at peripheral punctae. This accelerated transition from mature FAs to fibrillar adhesions was found not to result from any changes in total tensin-1 expression at 16 hours, however NRP2 depleted ECs were found to express significantly more tensin-1 at 90 minutes (Figure 4B-D).

Since an extended period of NRP2 depletion appeared to promote fibrillar adhesion formation, we asked whether this would also influence the polymerization and incorporation of secreted FN into its ECM. We immunolabeled siRNA-treated ECs fixed at 16 hours with antibodies against α5-integrin and extra domain-A (EDA)-containing cellular FN (EDA FN), which has previously been employed to examine cell secreted FN specifically.[15,52] Confocal microscopy revealed that NRP2 silencing significantly increased EDA-FN secretion from the cell body and from the ends of fibrillar adhesions. We subsequently assessed the relative quantity of incorporated polymerized EDA-FN in lysates collected from both Ctrl and NRP2 siRNA treated ECs biochemically, and found that NRP2 depleted ECs exhibited significantly increased levels of insoluble EDA-FN (Figure 4E-G). We therefore infer that the initial aberrations in α5-integrin trafficking and FA turnover rate elicited by loss of NRP2 force FAs to instead mature at an accelerated rate into fibrillar adhesions. This is accompanied by a concomitant surge in FN fibrillogenesis.

It is worth noting, however, that when siRNA-treated ECs were allowed to adhere for 48 hours, we did not observe any differences in EDA-FN secretion or α5-integrin morphology (Figure 4E,H-I), suggesting that any aberration elicited from NRP2 silencing becomes compensated for by this timepoint.

3.5 | Loss of endothelial NRP2 inhibits tumor angiogenesis in vivo

Upregulations in FAK activity giving rise to aggressive tumor phenotypes has been well substantiated.[54-57] FA assembly and subsequent FAK phosphorylation events in turn play a crucial role in FA turnover and remodeling of the actin cytoskeleton to promote cancer cell metastasis.[58] NRP2 overexpression is also known to promote tumorigenicity and metastasis in a multitude of cancer subtypes. It therefore represents a potential diagnostic or prognostic biomarker and therapeutic target for inhibiting primary tumor growth.[59] Despite this, little investigation into its contribution during tumor vascularization has been made. To isolate the role of NRP2 during tumor angiogenesis, we crossed NRP2-floxed (NRP2$^{fl/fl}$)-mice to tamoxifen (OHT)-inducible PDGFb-iCreERT2 mice and examined the effect of an acute EC-specific depletion of NRP2 on subcutaneous allograft tumor growth using CMT19T lung carcinoma cells. Cells were allowed to grow for a period of 18 d alongside thrice weekly injections of tamoxifen to effectively deplete NRP2 expression within the tumor vasculature (Figure 5A), avoiding the complications of interpreting NRP2 function using global knockout models. By tracking changes in tumor volume from day 10 post implantation, it was also possible to examine any temporal limitations to depleting NRP2 in this manner.

Tumors grown in NRP2^{flfl}.PDGFb-iCreERT2-positive (Cre-positive) animals developed significantly smaller than their control littermate NRP2^{flfl} (Cre-negative) counterparts despite no gross changes in mean animal weight (Figure 5B,C, Figure S3A). To directly assess the effects of EC-depletion of NRP2 on tumor angiogenesis, we performed immunofluorescent analysis on all tumors harvested from Cre-negative and Cre-positive mice. After confirming endothelial specific

depletion of NRP2 within endomucin-positive blood vessels in Cre-positive tumor sections (Figure 5D), we found that compared to tumors from Cre-negative animals, those deficient in endothelial NRP2 displayed significantly less vasculature (Figure 5E,F). This indicates that the suppressed tumor growth and reduced tumor angiogenesis we observe in Cre-positive mice likely results from a NRP2-specific, EC-intrinsic defect.

3.6 | Deficiency of endothelial NRP2 transiently impairs neonatal retinal vascular development

While pathological and physiological angiogenesis are both driven by many of the same processes and stimuli, tumor vasculature is very much distinct from physiological vasculature. In addition to their highly tortuous organization, vessels that

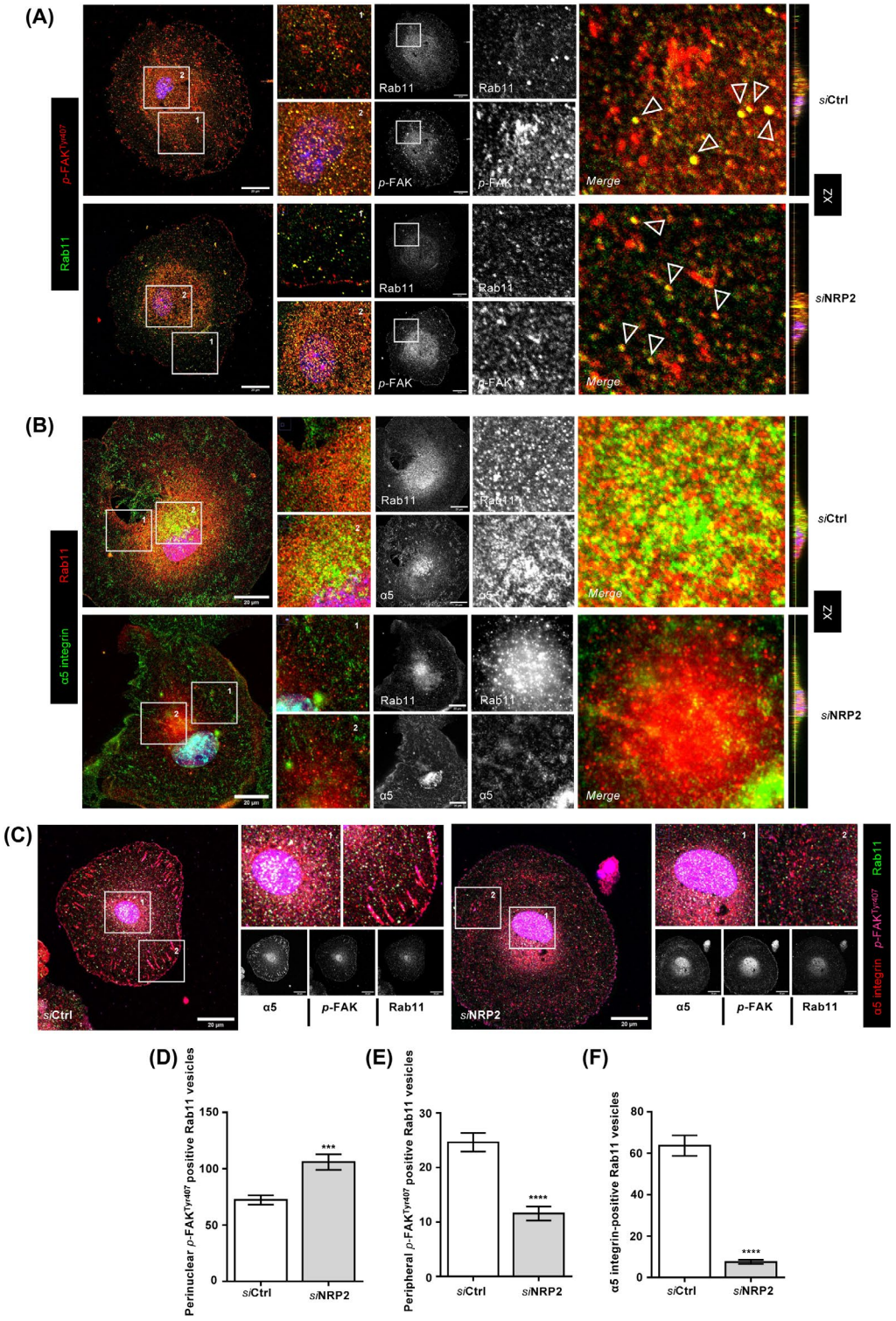

FIGURE 3 NRP2 regulates a α5-integrin- *p*-FAK^{Tyr407}-Rab11 trafficking axis. A, siRNA-transfected ECs were seeded onto FN coated coverslips and allowed to adhere for 90 min at 37°C and 5% CO_2 before being fixed. ECs were then co-immunostained for *p*-FAK (Tyr407) and Rab11. Images were taken using a Zeiss LSM880 Airyscan Confocal microscope at 63X magnification. Arrowheads show colocalization. XZ plane images for each panel are also shown to display subcellular colocalization. B, As described in (A), ECs were co-immunostained for α5-integrin and Rab11. C, As described in (A) ECs were co-immunostained for α5-integrin, *p*-FAK (Tyr407) and Rab11. D, Quantification of the mean number of perinuclear *p*-FAK (Tyr407)-positive Rab11 vesicles per 3x regions of interest (ROIs) between Ctrl siRNA and NRP2 siRNA-treated ECs. Error bars show ±SEM; n ≥ 10 cells/siRNA-treated group. Asterisks indicate statistical significance from an unpaired two-tailed *t* test. E, Quantification of the mean number of peripheral *p*-FAK (Tyr407)-positive Rab11 vesicles per 3x regions of interest (ROIs) between Ctrl siRNA and NRP2 siRNA-treated ECs. Error bars show ±SEM; n ≥ 10 cells/siRNA-treated group. Asterisks indicate statistical significance from an unpaired two-tailed *t* test. F, Quantification of the mean number of α5-integrin-positive Rab11 vesicles per cell between Ctrl siRNA and NRP2 siRNA-treated ECs. Error bars show ±SEM; N = 3 independent experiments; n ≥ 35 cells/siRNA-treated group. Asterisks indicate statistical significance from an unpaired two-tailed *t* test

form during tumorigenesis are far leakier than those that form under physiological homeostasis.[60,61] Studying the effects of depleting endothelial NRP2 in a physiological model was therefore necessary to obtain any mechanistic insight into its function during developmental angiogenesis. To this end, we utilized the postnatal mouse retina to examine whether any defect arose from inducing EC-specific depletion of NRP2 at postnatal day 6 (P6) or P12, timepoints during which the superficial plexus and the deep plexus are forming respectively.[62] Following tamoxifen administration regimens, we first confirmed successful depletion of NRP2 by co-staining with the endothelial marker BS-1 lectin in retinas harvested from Cre-negative and Cre-positive mice (Figure 6A).

The expression of NRP2 is largely considered to be more venous than arterial within the endothelium.[63,64] We were therefore unsurprised to observe enriched NRP2 expression within veins of the superficial plexus by co-immunolabeling with α-smooth muscle actin (α-SMA), a marker of smooth muscle cells that are known to primarily ensheathe arteries.[65] We also detected NRP2 expression in the disseminating microvasculature of the superficial plexus, particularly at the vascular front. Subsequent multi-plexus analysis revealed, however, very little NRP2 expression in the deep vascular layer at P12, suggesting that NRP2 plays a more prominent role during initial vessel sprouting outwards from the optic nerve to the retinal periphery rather than during deep plexus development (Figure 6A,B). To examine this further, we compared the vascular extension from the optic nerve between retinas harvested from Cre-negative and Cre-positive mice and found that EC-specific depletion of NRP2 significantly reduced radial expansion of the vasculature at P6 without affecting vessel density. By comparing the vascular extension of WT and PDGFb-iCreERT2-positive (Cre-only) retinas harvested at P6, and observing no significant differences (Figure S4A,B), we also confirmed that this phenotype did not arise due to Cre-toxicity.[66] Cre-positive retinas were also found to exhibit fewer sprouting ECs at the vascular front, consistent with NRP2's expression profile in Cre-negative retinas within the superficial layer (Figure 6C-H). Co-staining between BS-1 lectin and collagen IV also revealed that Cre-positive retinas exhibited significantly more vessels undergoing regression within the superficial plexus. This, paired with a significant reduction in vessel diameter, suggests that the vasculature of Cre-positive mice (Figure S4C-E) is less functional than that of their Cre-negative counterparts.

While the existence of FA structures in the developing postnatal retina is disputed, it has been demonstrated that FA-associated signaling cascades do exist.[37,67] In an attempt to corroborate our in vitro findings, we sought to examine differential FAK phosphorylation in the retina of our NRP2 deficient mice. Confocal microscopy of retinas harvested at P6 revealed that *p*-FAK^{Tyr407} staining was greatest at the vascular front and enriched at the apical ends of sprouting tip cells. *p*-FAK^{Tyr407} was also detected along the length of extending filopodia. However, in retinas harvested from Cre-positive mice, the relative intensity of *p*-FAK^{Tyr407} staining in sprouting tip cells was significantly diminished (Figure 6I,J). Taken together, this suggests that the reduced vascular extension and increased vascular regression we observe following NRP2 depletion, likely results from the inability of NRP2-deficient ECs to form stable cell-matrix interactions.

Defects at P6 were found to be transient however, as at P12, retinas from both Cre-negative and Cre-positive mice exhibited fully vascularized superficial plexus layers, with no gross differences in vessel density (Figure S4F-I). As we detected far less robust levels of NRP2 expression in the deep plexus layer of Cre-negative retinas compared to at the superficial plexus, we were also unsurprised to see the development of a normal vascular bed at the deep plexus layer in Cre-positive mice (Figure S4J-K). These data suggest that NRP2 is primarily involved in promoting initial EC sprouting and vascularization of the superficial plexus rather than during deep plexus development.

4 | DISCUSSION

When considered in conjunction with their interactions with other receptors known to regulate angiogenesis, such as α5β1- and αvβ3-integrins, the evidence purporting both NRPs as pro-angiogenic molecules holds true. For example, Valdembri et al, have previously reported that NRP1

promotes α5β1-integrin-mediated adhesion to FN matrices by selectively stimulating its rapid endocytosis from fibrillar adhesions and subsequent Rab5-dependent recycling to drive FA turnover in ECs.[16] Similarly, both we and others have demonstrated that NRP2 promotes cellular adhesion and migration *via* its interactions with the α5-integrin subunit.[24,68] Further evidence for this has recently been provided by Luo et al, who demonstrated that NRP2 may regulate migration by upregulating cofilin activity, a key mediator of actin depolymerization at slow growing filament ends.[35] Here, we provide evidence that NRP2 associates with a number of other proteins known to stabilize and promote actin branch nucleation and stress fiber growth, notably cortactin, VASP and fascin.[38-41] It is likely therefore, that NRP2 drives the simultaneous depolymerization of F-actin at slow-growing filament ends to supply the demand for new actin monomers at assembling fast growing ends of extending filopodial protrusions. NRP2-mediated VASP phosphorylation in

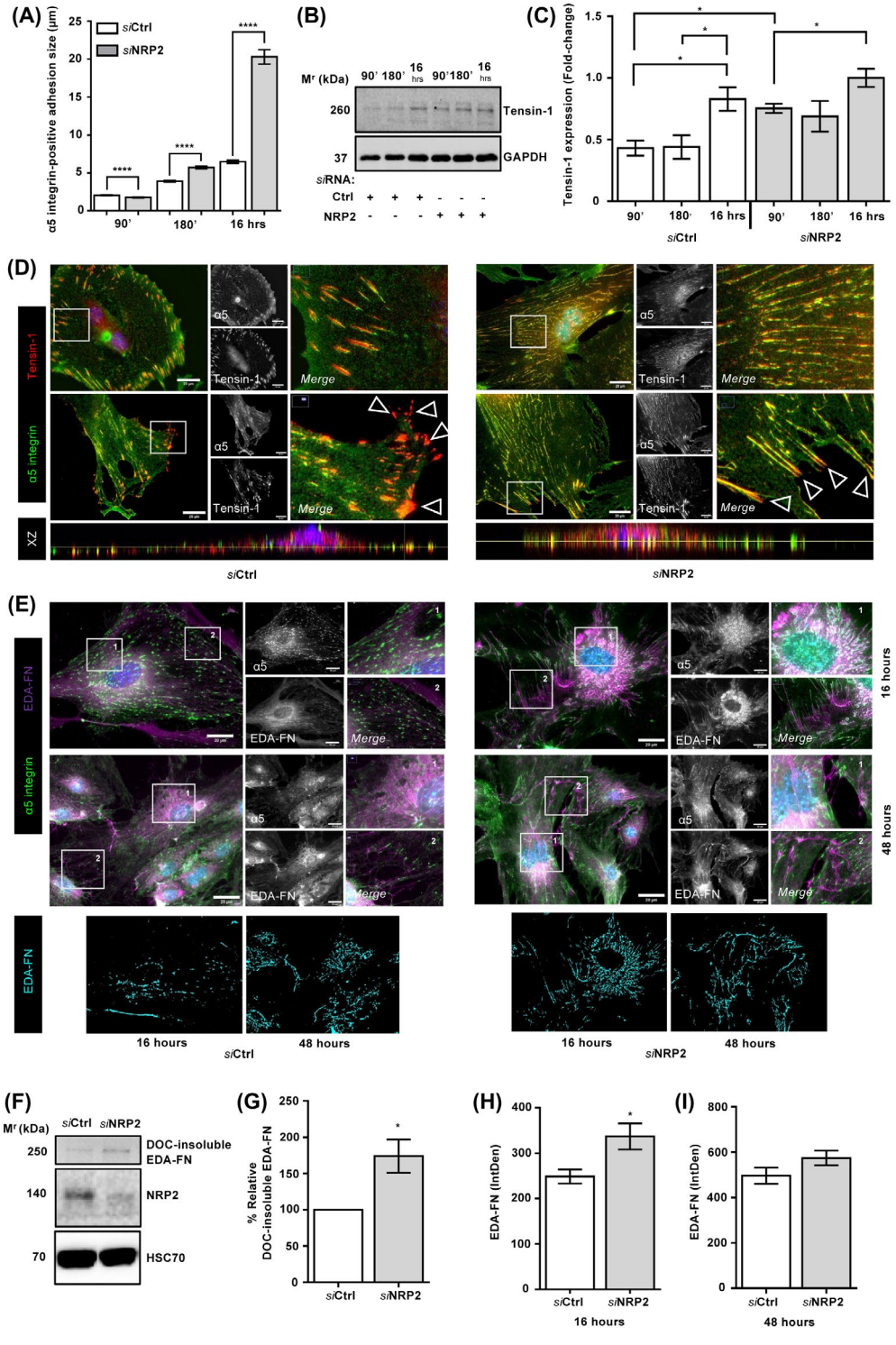

FIGURE 4 Long term depletion of NRP2 accelerates FA maturation and fibrillogenesis. A, Mean length of α5-integrin adhesions (μm), error bars show mean ± SEM; n ≥ 150 adhesions/timepoint/condition); Asterisks indicate statistical significance from an unpaired two-tailed *t* test. B, siRNA-transfected ECs were seeded onto 6 cm dishes pre-coated with 10 μg/mL FN and incubated for either 90, 180 min or 16 h at 37°C. ECs were lysed in ESB and subjected to the DC protein assay before being analyzed by western blotting using primary antibodies against Tensin-1. GAPDH was used as a loading control. C, Bands were quantified using ImageJ densitometric analysis. Error bar shows mean ± SEM; N = 3 independent experiments; asterisks indicate statistical significance from an unpaired two-tailed *t* test. D, siRNA-transfected ECs were seeded onto FN coated coverslips and allowed to adhere for 16 h at 37°C and 5% CO_2 before being fixed. ECs were co-immunostained for α5-integrin and tensin-1. Images were taken using a Zeiss LSM880 Airyscan Confocal microscope at 63X magnification. XZ plane images for each panel are also shown to display colocalization. E, As described in D), ECs were allowed to adhere for either 16 for 48 h, before being co-immunolabeled with α5-integrin and EDA-FN. F, siRNA-treated ECs were allowed to adhere for 16 h at 37°C and 5% CO_2. ECs were then lysed, cleared and the insoluble fraction isolated. Insoluble fractions were separated by SDS-PAGE and subjected to Western blot analysis. Membranes were incubated in anti-EDA-FN primary antibody to assess quantities of insoluble cell secreted FN, anti-NRP2 primary antibody to confirm NRP2 depletion, and anti-HSC70 antibody as a loading control. G, % insoluble EDA-FN. Mean densitometric analysis obtained using ImageJ. Error bars show mean ± SEM; N ≥ 3 independent experiments; asterisks indicate statistical significance from an unpaired two-tailed test. H/I, Quantification of EDA-FN density at either 16 h (H) or 48 h (I) adhesion to FN. Error bars show mean ± SEM; n ≥ 20 ECs/group. Asterisks indicate statistical significance from an unpaired two-tailed *t* test

turn potentiates the rapid polymerization and nucleation of F-actin at fast growing ends by initiating the translocation and activation of Rac1 to newly forming adhesions.

It is known that aberrations in VASP activity result in reduced FAK phosphorylation. For example, VASP inhibition has been shown to significantly reduce phosphorylation at Tyr-925 in a human chronic myeloid leukemia (CML) cell line, and decrease Tyr^{397} phosphorylation during *Xenopus* somite development.[44,69] As VASP is strongly Ser^{157} phosphorylated at FAs,[41,43] we were unsurprised to observe a corresponding significant reduction in FAK phosphorylation at Tyr^{397} and Tyr^{407} sites, both implicated in canonical VEGF gradient-driven EC adhesion and migration through their necessity for correct assembly of nascent FAs. VEGF-mediated phosphorylation of FAK at its Tyr^{407} residue during integrin-directed adhesion and migration is also known to be NRP1 dependent.[11,47] While NRP2 has been shown to direct FAK-mediated adhesion in cancerous epithelial cells via α6β1,[45] and to support branching morphogenesis in the developing mammary gland,[46] no connection has been explored in microvascular ECs. Endogenous *p*-FAK^{Tyr407} staining in fixed ECs subsequently revealed that significantly less phosphorylated FAK appears to be recruited to α5-integrin positive adhesion sites following NRP2 knockdown, resulting in smaller less developed FAs. Given we have previously provided evidence to suggest that NRP2 exerts a mainly VEGF-independent role during EC adhesion and migration,[24] we propose that NRP2 instead promotes FAK auto-phosphorylation following integrin engagement and clustering.

As NRP2 silencing disrupted Rab11-directed recycling of α5-integrin-*p*-FAK complexes back to assembling nascent adhesions, it is likely that NRP2 potentiates FAK-mediated signaling cascades by regulating the pool of available α5β1-integrin capable of binding the FN matrix. In support of this, studies have purported that α5-integrin is maintained in an active, unliganded conformation when endocytosed with active FAK, and during Rab11-mediated recycling.[34] This then enables more efficient integrin engagement with the matrix, and subsequent reassembly of polarized FAs to promote directional migration. As we observed a significant loss in colocalization between *p*-FAK^{Tyr407} and α5-integrin within $Rab11^+$ vesicles, concomitant with an accumulation of *p*-FAK^{Tyr407} at the perinuclear region, we infer that NRP2 is involved in maintaining the interactions between active FAK and α5-integrin during vesicular transport.

To our surprise, protracted siRNA-mediated depletion of NRP2 accelerated the transition from mature FAs to tensin-1 positive fibrillar adhesions translocating α5-integrin to the cell body. We believe this to be an artifact arising from aberrations in FA turnover rate, whereby FAs are forced to mature prematurely rather than be dynamically endocytosed and recycled. To confirm this model, we examined the effects of NRP2 silencing on the assembly of fibrillar FN. This remodeling of the extracellular matrix is driven by the actomyosin tension accrued from the translocation of α5β1 integrin into fibrillar adhesions and is essential during angiogenesis for vessel formation.[52] Contemporaneous to the surge in fibrillar adhesion formation we observed in our NRP2 depleted ECs fixed at 16 hours, immunostaining and deoxycholate (DOC)-buffer extracted insoluble EDA-FN quantification revealed a surge in secreted FN radiating outwards from α5-integrin containing adhesions. In support of these findings, others have established that Rab11-mediated recycling of α5-integrin orchestrates the continuous renewal of polarized FN fibrils being secreted to form an extracellular fibrillar network.[15,52] We propose here that the early defects in FA turnover rate elicited by NRP2 depletion, although eventually compensated for, sustains the transition to a more sedentary cell fate in which the premature development of fibrillar adhesions promotes the integration of secreted FN into insoluble fibrils. By doing so, stability and contractility is favored over motility. Alongside other studies,[70] this work reinforces the growing evidence in multiple cell types that NRP2 deficiency can promote cell contractility.

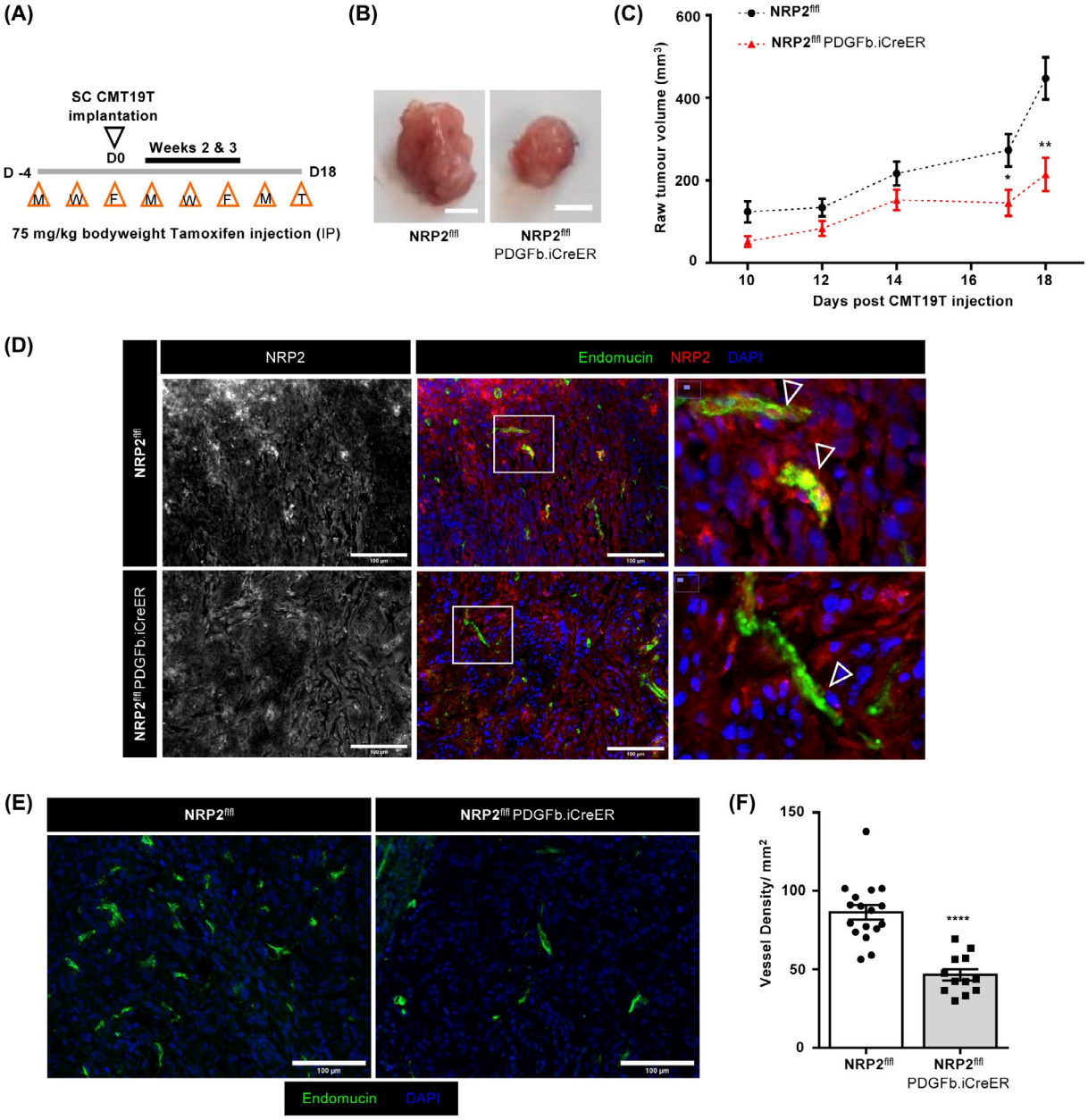

FIGURE 5 Loss of endothelial NRP2 inhibits tumor angiogenesis in vivo. Inducible, endothelial specific deletion of NRP2 was achieved by crossing mice expressing the PDGFb.iCreER promoter of Cre-recombinase to those floxed for NRP2. A, Experimental schematic: tamoxifen-induced activation of Cre-recombinase and thus deletion of NRP2 was employed via the following regimen in order to study its role during tumorigenesis. $NRP2^{fl/fl}$; PDGFb.iCreER (Cre-positive) and $NRP2^{fl/fl}$ (Cre-negative) littermate control mice received intraperitoneal (IP) injections of tamoxifen (75 mg/kg bodyweight) thrice weekly (Monday, Wednesday, Friday) for the duration of the experiment from D-4 to D17 to induce Cre-recombinase activity. CMT19T lung carcinoma cells (1 × 106) were implanted subcutaneously (SC) into the flank of mice at D0 and allowed to grow until D18. B, Representative images of tumors harvested from Cre-negative and Cre-positive mice at day 18. C, Quantification of tumor volumes measured from tumor bearing Cre-negative and Cre-positive mice measured between day 10 and day 18 post CMT19T injection. Error bars show mean ± SEM; N = 3 independent experiments; n ≥ 12 tumors per genotype. Asterisks indicate statistical significance from an unpaired two-tailed *t* test. D, IHC staining using Endomucin and NRP2 primary antibodies to confirm endothelial specific NRP2 deletion in blood vessels from Cre-positive tumors. E, Representative tumor sections from Cre-negative and Cre-positive tumors showing endomucin-positive blood vessels. F, Quantification of number of blood vessel density per mm^2. Mean quantification performed on 3x ROIs per tumor section, from 3x sections per tumor. Error bars show mean ± SEM; N = 3 independent experiments; n ≥ 12. Asterisks indicate statistical significance from an unpaired two-tailed *t* test

In an effort to emphasize the relevance of endothelial NRP2 during angiogenesis and its coordination of α5-integrin trafficking in vivo, we modeled the effects of its EC specific depletion during both pathological and physiological vessel growth. While it has been substantiated by many that NRP2 promotes a more aggressive cancer phenotype,[59]

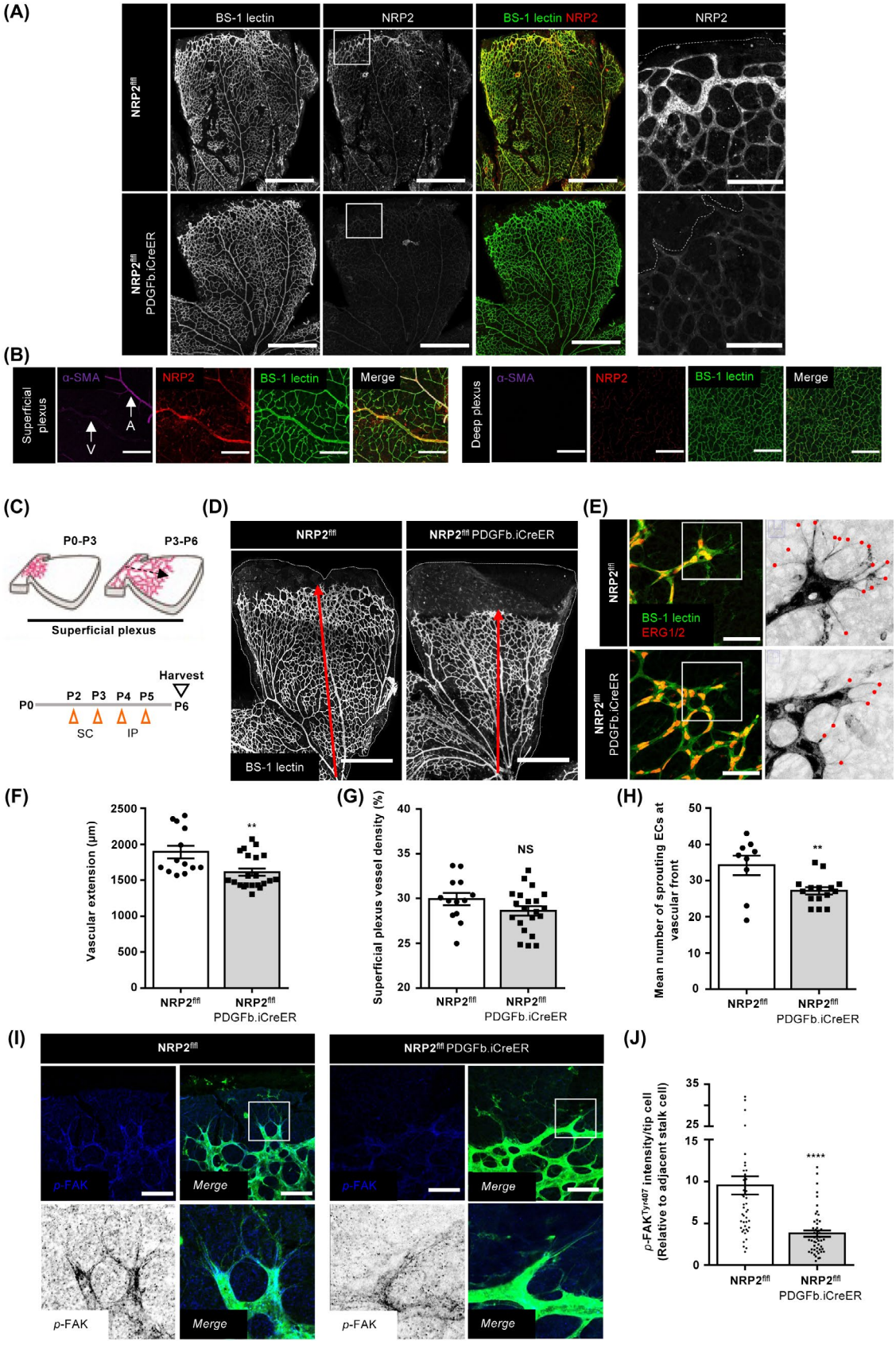

FIGURE 6 Deficiency of endothelial NRP2 transiently impairs neonatal retinal vascular development. Inducible, endothelial specific deletion of NRP2 was achieved by crossing mice expressing the PDGFb.iCreER promoter of Cre-recombinase to those floxed for NRP2. A, Tamoxifen-induced NRP2 deletion was confirmed by co-staining NRP2 with BS1-lectin. Scale bar = 500 μm. B, Representative images of BS-1 lectin-, α-SMA-, and NRP2-labeled vasculature from Cre-negative and Cre-positive retinas harvested at P6 and P12. Panels show superficial and deep plexus layers. Scale bar = 150 μm. C, Experimental schematic: tamoxifen-induced activation of Cre-recombinase and thus deletion of NRP2 was employed via the following regime in order to study its role during the formation of the developing retinal superficial vascular plexus. Cre-positive and Cre-negative littermate control mice received subcutaneous (SC) injections of tamoxifen (50 μL, 2 mg/mL stock) on postnatal (P) days 2 and 3, followed by intraperitoneal (IP) injections of the same dose on P4 and 5. Retinas were then harvested at P6 (Figure adapted from Milde et al[62]). D, Representative images of BS-1 lectin-labeled P6 retinas harvested from Cre-negative and Cre-positive mice showing vascular extension from the optic nerve. Scale bar = 500 μm. E, Representative images of BS-1 lectin and ERG1/2 co-labeled P6 retinas showing sprouting ECs at the vascular front. Scale bar = 50 μm. Gray scale images show magnified ROIs from left panels, with filopodial extensions highlighted in red. F, Quantification of P6 vascular extension from the optic nerve, presented as raw values. Error bars show mean ± SEM; N = 3 independent experiments; n ≥ 13 retinas. Asterisks indicate statistical significance from an unpaired two-tailed *t* test. G, Quantification of mean % vessel density from 350x350 μm ROIs taken per leaf of each P6 retina. Error bars show mean ± SEM; N = 3 independent experiments; n ≥ 13 retinas. NS stands for non-significance from an unpaired two-tailed *t* test. H, Quantification of the mean number of sprouting ECs per retina leaf. Error bars show mean ± SEM; N = 2 independent experiments; n ≥ 10 retinas. Asterisks indicate statistical significance from an unpaired two-tailed *t* test. I, Representative images of *p*-FAK Tyr-407-labeled retinal vasculature co-labeled with BS-1 lectin from Cre-negative and Cre-positive mice at P6. Scale bar = 50 μm. J, Quantification of *p*-FAK Tyr-407 intensity within sprouting tip cells made relative to adjacent stalk cell intensities. Error bars show mean ± SEM; n ≥ 50 tip cells); ****P <.0001, unpaired students *t* test (two-tailed)

our findings clearly demonstrate that the expansion of tumor vasculature to support primary tumor growth is inhibited following loss of endothelial NRP2. Likewise, in the developing retina, vascular outgrowth from the optic nerve at P6 is impaired in animals depleted in endothelial NRP2. NRP2 is largely considered to be expressed to a greater extent within veins as opposed to arteries,[63] however, little is known about its expression profile or its endothelial-specific contributions during the hierarchical vascularization of the postnatal retina. Studies have shown that NRP2 does not compensate for the loss of NRP1's cytoplasmic domain during retina development and arterial/venous differentiation.[64] Indeed, the published evidence outlining the roles of the neuropilins during angiogenesis support the principle that NRP1 likely plays a more dominant role over NRP2. Despite this, we found that vascular extension within the superficial plexus was significantly impaired following NRP2 depletion at P6, owing to a decrease in the number of sprouting tip cells at the vascular front. These defects were found to likely arise from a deficiency in polarized FA-associated signaling, specifically FAK phosphorylation within sprouting tip cells, which has been previously alluded to be responsible for the formation of stable cell-matrix interactions.[67] These findings align with the expression profile of NRP2, which showed a far more robust expression at the vascular front of the superficial plexus, compared to within the deep plexus layer.

Taken together, these data presented provide evidence that endothelial NRP2 plays a key role in regulating both pathological and physiological angiogenesis. We propose a model whereby NRP2 promotes FA development by regulating α5-integrin trafficking and show that NRP2 is essential for vessel development by enabling the formation of stable cell-matrix connections.

ACKNOWLEDGMENTS

This work was supported by funding from: the UKRI Biotechnology and Biological Sciences Research Council Norwich Research Park Biosciences Doctoral Training Partnership and BHF (grant number PG/15/25/31369). Additionally, we thank Norfolk Fundraisers, Mrs Margaret Doggett, and the Colin Wright Fund for their kind support and fundraising over the years. Robinson is also partially funded by the BBSRC Institute Strategic Programme Gut Microbes and Health BB/R012490/1 and its constituent project (BBS/E/F/000PR10355).

CONFLICT OF INTEREST

All authors declare no conflicts of interest.

AUTHOR CONTRIBUTIONS

Conceptualization: C.J. Benwell, J.A.G.E. Taylor, S.D. Robinson; Formal analyses: C.J. Benwell, J.A.G.E. Taylor, S.D. Robinson; Investigation: C.J. Benwell, J.A.G.E. Taylor, S.D. Robinson; Resources: S.D. Robinsons; Review and editing: C.J. Benwell, J.A.G.E. Taylor, S.D. Robinson; Visualization: C.J. Benwell, J.A.G.E. Taylor, S.D. Robinson; Supervision: S.D. Robinson; Funding acquisition: S.D. Robinson.

ORCID

Stephen D. Robinson https://orcid.org/0000-0002-6606-7588

REFERENCES

1. Hanahan D, Weinberg RA. Hallmarks of cancer: the next generation. *Cell*. 2011;144(5):646-674. https://doi.org/10.1016/j.cell.2011.02.013

2. Robinson SD, Hodivala-Dilke KM. The role of β3-integrins in tumor angiogenesis: context is everything. *Curr Opin Cell Biol*. 2011;23(5):630-637. https://doi.org/10.1016/j.ceb.2011.03.014
3. Calderwood DA. Integrin activation. *J Cell Sci*. 2004;117(5):657-666. https://doi.org/10.1242/jcs.01014
4. Pan LI, Zhao Y, Yuan Z, et al. Research advances on structure and biological functions of integrins. *SpringerPlus*. 2016;5(1): https://doi.org/10.1186/s40064-016-2502-0
5. Woodside D, Liu S, Ginsberg M. Integrin activation. *Thromb Haemost*. 2001;86:316-323.
6. Buskermolen ABC, Kurniawan NA, Bouten CVC. An automated quantitative analysis of cell, nucleus and focal adhesion morphology. *PLoS One*. 2018;13(3):1-16. https://doi.org/10.1371/journal.pone.0195201
7. Hu P, Luo BH. Integrin bi-directional signaling across the plasma membrane. *J Cell Physiol*. 2013;228(2):306-312. https://doi.org/10.1002/jcp.24154
8. Hynes R. Integrins: bidirectional allosteric signaling machines. *Cell*. 2002;110:673-687. https://www.ncbi.nlm.nih.gov/pubmed/12297042
9. De Pascalis C, Etienne-Manneville S. Single and collective cell migration: the mechanics of adhesions. *Mol Biol Cell*. 2017;28(14):1833-1846. https://doi.org/10.1091/mbc.E17-03-0134
10. Srichai M, Zent R. *Integrin Structure and Function: Cell-Extracellular Matrix Interactions in Cancer*. Boston, MA: Springer; 2010.
11. Chang F, Lemmon CA, Park D, Romer LH. FAK potentiates Rac1 activation and localization to matrix adhesion sites: a role for beta-PIX. *Mol Biol Cell*. 2007;18:253-264.
12. Sadok A, Marshall CJ. Rho gtpases masters of cell migration. *Small GTPases*. 2014;5(4):e983878. https://doi.org/10.4161/sgtp.29710
13. Goley E, Welch M. The ARP2/3 complex: an actin nucleator comes of age. *Nat Rev Mol Cell Biol*. 2006;7:713-726.
14. Kaksonen M, Toret CP, Drubin DG. Harnessing actin dynamics for clathrin-mediated endocytosis. *Nat Rev Mol Cell Biol*. 2006;7(6):404-414. https://doi.org/10.1038/nrm1940
15. Sundararaman A, Fukushima Y, Norman JC, et al. RhoJ regulates α5β1 integrin trafficking to control fibronectin remodeling during angiogenesis. *Curr Biol*. 2020;30(11):2146-2155.e5. https://doi.org/10.1016/j.cub.2020.03.042
16. Valdembri D, Caswell PT, Anderson KI, et al. Neuropilin-1/GIPC1 signaling regulates α5β1 integrin traffic and function in endothelial cells. *PLoS Biol*. 2009;7(1):e1000025. https://doi.org/10.1371/journal.pbio.1000025
17. Fakhari M, Pullirsch D, Abraham D, et al. Selective upregulation of vascular endothelial growth factor receptors neuropilin-1 and -2 in human neuroblastoma. *Cancer*. 2002;94(1):258-263. https://doi.org/10.1002/cncr.10177
18. Kawakami T, Tokunaga T, Hatanaka H, et al. Neuropilin 1 and neuropilin 2 co-expression is significantly correlated with increased vascularity and poor prognosis in nonsmall cell lung carcinoma. *Cancer*. 2002;95(10):2196-2201. https://doi.org/10.1002/cncr.10936
19. Bielenberg DR, Hida Y, Shimizu A, et al. Semaphorin 3F, a chemorepulsant for endothelial cells, induces a poorly vascularized, encapsulated, nonmetastatic tumor phenotype. *J Clin Invest*. 2004;114(9):1260-1271. https://doi.org/10.1172/JCI200421378.1260
20. Lantuéjoul S, Constantin B, Drabkin H, et al. Expression of VEGF, semaphorin SEMA3F, and their common receptors neuropilins NP1 and NP2 in preinvasive bronchial lesions, lung tumours, and cell lines. *J Pathol*. 2003;200(3):336-347. https://doi.org/10.1002/path.1367
21. Vales A, Kondo R, Aichberger KJ, et al. Myeloid leukemias express a broad spectrum of VEGF receptors including neuropilin-1 (NRP-1) and NRP-2. *Leuk Lymphoma*. 2007;48(10):1997-2007. https://doi.org/10.1080/10428190701534424
22. Bachelder RE, Crago A, Chung J, et al. Vascular endothelial growth factor is an autocrine survival factor for neuropilin-expressing breast carcinoma cells. *Can Res*. 2001;61(15):5736-5740.
23. Fukahi K, Fukasawa M, Neufeld G, et al. Aberrant expression of neuropilin-1 and -2 in human pancreatic cancer cells. *Clin Cancer Res*. 2004;10(2):581-590. https://doi.org/10.1158/1078-0432.CCR-0930-03
24. Alghamdi AAA, Benwell CJ, Atkinson SJ, et al. NRP2 as an emerging angiogenic player; promoting endothelial cell adhesion and migration by regulating recycling of α5 integrin. *Front Cell Dev Biol*. 2020;8(May):1-16. https://doi.org/10.3389/fcell.2020.00395
25. Favier B, Alam A, Barron P, et al. Neuropilin-2 interacts with VEGFR-2 and VEGFR-3 and promotes human endothelial cell survival and migration. *Blood*. 2006;108(4):1243-1250. https://doi.org/10.1182/blood-2005-11-4447
26. Plein A, Fantin A, Ruhrberg C. Neuropilin regulation of angiogenesis, arteriogenesis, and vascular permeability. *Microcirculation*. 2014;21(4):315-323. https://doi.org/10.1111/micc.12124
27. Reynolds L, Hodivala-Dilke K. Primary mouse endothelial cell culture for assays of angiogenesis. *Methods Mol Med*. 2006;120:503-509.
28. Robinson SD, Reynolds LE, Kostourou V, et al. Avβ3 integrin limits the contribution of neuropilin-1 to vascular endothelial growth factor-induced angiogenesis. *J Biol Chem*. 2009;284(49):33966-33981. https://doi.org/10.1074/jbc.M109.030700
29. Krilleke D, DeErkenez A, Schubert W, et al. Molecular mapping and functional characterization of the VEGF164 heparin-binding domain. *J Biol Chem*. 2007;282(38):28045-28056. https://doi.org/10.1074/jbc.M700319200
30. Lambert J, Makin K, Akbareian S, et al. ADAMTS-1 and syndecan-4 intersect in the regulation of cell migration and angiogenesis. *J Cell Sci*. 2020;133(7):1-15. https://doi.org/10.1242/jcs.235762
31. Clark RAF, DellaPelle P, Manseau E, et al. Blood vessel fibronectin increases in conjunction with endothelial cell proliferation and capillary ingrowth during wound healing. *J Invest Dermatol*. 1982;79(5):269-276. https://doi.org/10.1111/1523-1747.ep12500076
32. Ingber DE. Fibronectin controls capillary endothelial cell growth by modulating cell shape. *Proc Natl Acad Sci U S A*. 1990;87(9):3579-3583. https://doi.org/10.1073/pnas.87.9.3579
33. Bökel C, Brown NH. Integrins in development: moving on, responding to, and sticking to the extracellular matrix. *Dev Cell*. 2002;3(3):311-321. https://doi.org/10.1016/S1534-5807(02)00265-4
34. Nader GPF, Ezratty EJ, Gundersen GG. FAK, talin and PIPKI 3 regulate endocytosed integrin activation to polarize focal adhesion assembly. *Nat Cell Biol*. 2016;18(5):491-503. https://doi.org/10.1038/ncb3333
35. Luo XI, He J-Y, Xu J, et al. Vascular NRP2 triggers PNET angiogenesis by activating the SSH1-cofilin axis. *Cell Biosci*. 2020;10(1):1-16. https://doi.org/10.1186/s13578-020-00472-6
36. Fantin A, Lampropoulou A, Gestri G, et al. NRP1 regulates CDC42 activation to promote filopodia formation in endothelial tip

cells. *Cell Rep*. 2015;11(10):1577-1590. https://doi.org/10.1016/j.celrep.2015.05.018

37. Raimondi C, Fantin A, Lampropoulou A, et al. Imatinib inhibits VEGF-independent angiogenesis by targeting neuropilin 1- dependent ABL1 activation in endothelial cells. *J Exp Med*. 2014;211(6):1167-1183. https://doi.org/10.1084/jem.20132330
38. Uruno T, Liu J, Zhang P, et al. Activation of Arp2/3 complex-mediated actin polymerization by cortactin. *Nat Cell Biol*. 2001;3(3):259-266. https://doi.org/10.1038/35060051
39. Woo MK, Fowler VM. Identification and characterization of tropomodulin and tropomyosin in the adult rat lens. *J Cell Sci*. 1994;107(5):1359-1367.
40. Yamakita Y, Ono S, Matsumura F, et al. Phosphorylation of human fascin inhibits its actin binding and bundling activities. *J Biol Chem*. 1996;271(21):12632-12638. https://doi.org/10.1074/jbc.271.21.12632
41. Benz PM, Blume C, Seifert S, et al. Differential VASP phosphorylation controls remodeling of the actin cytoskeleton. *J Cell Sci*. 2009;122(21):3954-3965. https://doi.org/10.1242/jcs.044537
42. Jalal S, Shi S, Acharya V, et al. Actin cytoskeleton self-organization in single epithelial cells and fibroblasts under isotropic confinement. *J Cell Sci*. 2019;132(5):1-14. https://doi.org/10.1242/jcs.220780
43. Holt MR, Critchley DR, Brindle NPJ. The focal adhesion phosphoprotein, VASP. *Int J Biochem Cell Biol*. 1998;30(3):307-311. https://doi.org/10.1016/S1357-2725(97)00101-5
44. Kragtorp KA, Miller JR. Regulation of somitogenesis by Ena/VASP proteins and FAK during Xenopus development. *Development*. 2006;133(4):685-695. https://doi.org/10.1242/dev.02230
45. Goel HL, Pursell B, Standley C, et al. Neuropilin-2 regulates α6β1 integrin in the formation of focal adhesions and signaling. *J Cell Sci*. 2012;125(2):497-506. https://doi.org/10.1242/jcs.094433
46. Goel HL, Bae D, Pursell B, et al. Neuropilin-2 promotes branching morphogenesis in the mouse mammary gland. *Development*. 2011;138(14):2969-2976. https://doi.org/10.1242/dev.051318
47. Herzog B, Pellet-Many C, Britton G, et al. VEGF binding to NRP1 is essential for VEGF stimulation of endothelial cell migration, complex formation between NRP1 and VEGFR2, and signaling via FAK Tyr407 phosphorylation. *Mol Biol Cell*. 2011;22(15):2766-2776. https://doi.org/10.1091/mbc.E09-12-1061
48. Schaller MD. Cellular functions of FAK kinases: Insight into molecular mechanisms and novel functions. *J Cell Sci*. 2010;123(7):1007-1013. https://doi.org/10.1242/jcs.045112
49. Michael KE, Dumbauld DW, Burns KL, et al. Focal adhesion kinase modulates cell adhesion strengthening via integrin activation. *Mol Biol Cell*. 2009;20(9):2508-2519. https://doi.org/10.1091/mbc.E08-01-0076
50. Ajeian JN, Horton ER, Astudillo P, et al. Proteomic analysis of integrin-associated complexes from mesenchymal stem cells. *Proteomics Clin Appl*. 2016;10(1):51-57. https://doi.org/10.1002/prca.201500033
51. Rossier O, Octeau V, Sibarita J-B, et al. Integrins β1 and β3 exhibit distinct dynamic nanoscale organizations inside focal adhesions. *Nat Cell Biol*. 2012;14(10):1057-1067. https://doi.org/10.1038/ncb2588
52. Mana G, Clapero F, Panieri E, et al. PPFIA1 drives active α5β1 integrin recycling and controls fibronectin fibrillogenesis and vascular morphogenesis. *Nat Commun*. 2016;7(November):13546. https://doi.org/10.1038/ncomms13546
53. Zamir E, Katz M, Posen Y, et al. Dynamics and segregation of cell-matrix adhesions in cultured fibroblasts. *Nat Cell Biol*. 2000;2(4):191-196. https://doi.org/10.1038/35008607
54. Gao C, Chen G, Kuan SF, Zhang DH, Schlaepfer DD, Hu J. FAK/PYK2 promotes the Wnt/β-catenin pathway and intestinal tumorigenesis by phosphorylating GSK3β. *eLife*. 2015;4:1-17. https://doi.org/10.7554/eLife.10072
55. Golubovskaya VM, Zheng M, Zhang LI, et al. The direct effect of Focal Adhesion Kinase (FAK), dominant-negative FAK, FAK-CD and FAK siRNA on gene expression and human MCF-7 breast cancer cell tumorigenesis. *BMC Cancer*. 2009;9:280. https://doi.org/10.1186/1471-2407-9-280
56. Zhang J, Hochwald SN. The role of FAK in tumor metabolism and therapy. *Pharmacol Ther*. 2014;142(2):154-163. https://doi.org/10.1016/j.pharmthera.2013.12.003
57. Lenzo FL, Cance WG. From tumorigenesis to microenvironment and immunoregulation: The many faces of focal adhesion kinase and challenges associated with targeting this elusive protein. *Transl Cancer Res*. 2017;6(17):S957-S960. https://doi.org/10.21037/tcr.2017.06.05
58. Nagano M, Hoshino D, Koshikawa N, et al. Turnover of focal adhesions and cancer cell migration. *Int J Cell Biol*. 2012;2012:1-10. https://doi.org/10.1155/2012/310616
59. Borkowetz A, Froehner M, Rauner M, et al. Neuropilin-2 is an independent prognostic factor for shorter cancer-specific survival in patients with acinar adenocarcinoma of the prostate. *Int J Cancer*. 2020;146(9):2619-2627. https://doi.org/10.1002/ijc.32679
60. Deshpande PP, Biswas S, Torchilin VP. Current trends in the use of liposomes for tumor targeting. *Nanomedicine*. 2013;8(9):1509-1528. https://doi.org/10.2217/nnm.13.118
61. Ghosh Dastidar D, Ghosh D, Chakrabarti G. Tumour vasculature targeted anti-cancer therapy. *Vessel Plus*. 2020;2020: https://doi.org/10.20517/2574-1209.2019.36
62. Milde F, Lauw S, Koumoutsakos P, et al. The mouse retina in 3D: Quantification of vascular growth and remodeling. *Integr Biol (Camb)*. 2013;5(12):1426-1438. https://doi.org/10.1039/c3ib40085a
63. Bielenberg D, Pettaway C, Takashima S, et al. Neuropilins in neoplasms: Expression, regulation, and function. *Exp Cell Res*. 2006;312(5):584-593. https://doi.org/10.1016/j.yexcr.2005.11.024
64. Fantin A, Schwarz Q, Davidson K, et al. The cytoplasmic domain of neuropilin 1 is dispensable for angiogenesis, but promotes the spatial separation of retinal arteries and veins. *Development*. 2011;138(19):4185-4191. https://doi.org/10.1242/dev.070037
65. Alarcon-Martinez L, Yilmaz-Ozcan S, Yemisci M, et al. Capillary pericytes express α-smooth muscle actin, which requires prevention of filamentous-actin depolymerization for detection. *eLife*. 2018;7:1-17. https://doi.org/10.7554/eLife.34861
66. Brash JT, Bolton RL, Rashbrook VS, Denti L, Kubota Y, Ruhrberg C. Tamoxifen-activated CreERT impairs retinal angiogenesis independently of gene deletion. *Circ Res*. 2020;127(6):849-850.
67. Schimmel L, Fukuhara D, Richards M, et al. C-Src controls stability of sprouting blood vessels in the developing retina independently of cell-cell adhesion through focal adhesion assembly. *Development*. 2020;147(7):dev185405. https://doi.org/10.1242/dev.185405
68. Cao Y, Hoeppner LH, Bach S, et al. Neuropilin-2 promotes extravasation and metastasis by interacting with endothelial α5 integrin. *Can Res*. 2013;73(14):4579-4590. https://doi.org/10.1158/0008-5472.CAN-13-0529
69. Bernusso VA, Machado-Neto JA, Pericole FV, et al. Imatinib restores VASP activity and its interaction with Zyxin in BCR-ABL

leukemic cells. *Biochim Biophys Acta*. 2015;1853(2):388-395. https://doi.org/10.1016/j.bbamcr.2014.11.008

70. Bielenberg DR, Seth A, Shimizu A, et al. Increased smooth muscle contractility in mice deficient for neuropilin 2. *Am J Pathol*. 2012;181(2):548-559. https://doi.org/10.1016/j.ajpath.2012.04.013

SUPPORTING INFORMATION

Additional Supporting Information may be found online in the Supporting Information section.

How to cite this article: Benwell CJ, Taylor JAGE, Robinson SD. Endothelial neuropilin-2 influences angiogenesis by regulating actin pattern development and α5-integrin-*p*-FAK complex recruitment to assembling adhesion sites. *The FASEB Journal*. 2021;35:e21679. https://doi.org/10.1096/fj.202100286R